ELSEVIER

Thin Solid Films 366 (2000) 150–154

thin solid films

www.elsevier.com/locate/tsf

# Medium-temperature plasma immersion-ion implantation of austenitic stainless steel

X.B. Tian, Z.M. Zeng, T. Zhang, B.Y. Tang, P.K. Chu*

*Department of Physics & Materials Science, City University of Hong Kong, 83 Tat Chee Avenue, Kowloon, Hong Kong*

Received 30 April 1999; received in revised form 11 January 2000; accepted 11 January 2000

**Abstract**

Conventional elevated-temperature plasma immersion-ion implantation (PIII) is usually conducted at 350°C, or above, to achieve a thick modified layer for practical engineering applications. In this paper, we focus on medium-temperature PIII treatment of SS304 stainless steel. Two experimental protocols: high frequency, low voltage (LV); and high voltage (HV), low frequency are evaluated. The samples are characterized by Auger electron spectroscopy, glancing angle X-ray diffraction (XRD), corrosion test, pin-on-disk friction and wear test, and so on, to determine the composition, phase structure, as well as the tribological properties of the modified layer. Our results indicate that PIII at 300°C not only improves the mechanical properties, but also the corrosion resistance. Comparison of the wear tracks shows that 300°C-PIII results in an 11-fold improvement in the surface-wear resistance. A procedure involving high implantation flux at LV is more favorable to the formation of a thick modified layer with a higher nitrogen concentration. 

*Keywords:* Steel; Plasma processing and deposition; Ion implantation; Tribology

## 1. Introduction

Plasma immersion-ion implantation (PIII) has recently emerged as a powerful surface-engineering technique to enhance the surface properties of materials and industrial components [1–5]. In order to achieve a thicker nitrided layer in metals, treatment at elevated temperature is usually preferred [6–10]. The targets are directly heated by the high-incident ion-flux during PIII, and the target temperature can be controlled by regulating the frequency and duration of the high-voltage pulses applied to the samples. The process combines conventional ion implantation and diffusion, and effectively produces the desirable near-surface microstructure which typically consists of an outer non-equilibrium layer, typical of nitrogen implantation, and a substantial diffusion zone of high nitrogen content.

Austenitic stainless steels, such as SS304 and SS316, possess relatively low hardness in the order of 200–300 kg/cm$^2$, and the large wear in abrasively-stressed parts leads to a short working lifetime. There are several processes to increase the surface hardness and reduce the wear, e.g. plasma nitriding and carburizing. However, due to slow diffusion and the existence of a surface chromium-rich barrier, these processes are usually operated at a high temperature in order to attain a treatment-depth of several micrometers in a reasonable time. In stainless steels, the high temperature (above 450°C) leads to the formation of chromium nitride, which binds chromium from the solid solution, thereby lowering the corrosion resistance of the materials. Recent work has shown that if nitriding is performed at or below 400°C, it is possible to obtain better surface properties. At this temperature, diffusion of interstitial nitrogen is still quite substantial, while the diffusion of substitutional chromium is prohibited, leading to a metastable supersaturated 'expanded austenite' phase. This has high hardness and good wear resistance on account of the compressive stress induced by the high nitrogen concentration. The chromium content does not precipitate as nitrides and remains in the solid solution allowing the formation of a protective oxide. PIII at or above 350°C and at a lower temperature [11,12] has been investigated, but very little work has been done at medium temperatures. In this paper, we focus on medium-temperature PIII at around 300°C. We also compare the effectiveness of two biasing voltages, 15 and 2 kV.

## 2. Experimental

A schematic of the PIII system [13] is shown in Fig. 1. A

* Corresponding author. Tel.: +852-2788-7724; fax: +852-2788-9549/7830.

*E-mail address:* paul.chu@cityu.edu.hk (P.K. Chu)

0040-6090/00/$ - see front matter 
PII: S0040-6090(00)00738-0

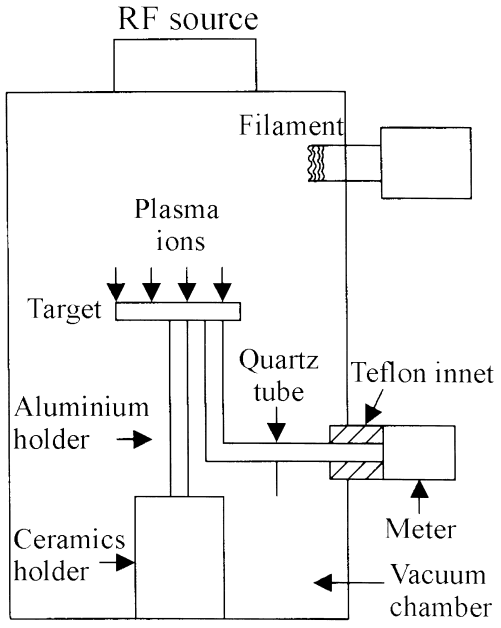


Fig. 1. Schematic of the PIII apparatus and the in-situ temperature-measurement set-up.

nitrogen plasma is ignited by four sets of hot filaments to achieve a uniform plasma in the vacuum chamber. The sample is heated by the incident ion-flux from the plasma when negative voltage pulses are applied. The heating rate depends on the bias voltage, plasma density, exposed surface area, pulse frequency, pulse duration, and heat removal or transfer rate. The sample temperature can thus be controlled by varying the pulsing frequency, or the filament current, to change the plasma density. The target temperature is monitored in-situ with an electrically-floating thermocouple connected directly to the target [14]. This temperature-measurement system has been shown to operate reliably, even in the presence of electrical arcing during the PIII process.

A SS304 stainless-steel bar, 25 mm in diameter, was cut into discs with a thickness of 4 mm. One surface of each sample was grounded and polished to a mirror finish, using standard metallographic techniques. The medium-temperature PIII experiments were conducted at two ion energies using two separate power modulators. For the 15-kV work, a conventional modulator was employed [13], whereas a newly-developed high frequency, low-voltage power modulator [15,16] was employed for the 2-kV process. The latter modulator can produce 35 kHz-square wave pulses, with a maximum voltage of 5 kV. Before each treatment process, 2 kV Ar plasma pre-cleaning was performed, and this step also raised the sample temperature to about 300°C. This provided a constant starting-temperature for each experiment to facilitate data comparison. The nitrogen working pressure was $2.0 \times 10^{-2}$ Pa, and the plasma density was adjusted between 1.0 and $4.0 \times 10^{9}$ ions/cm$^3$ to maintain a constant sample temperature. The other PIII instrumental parameters are shown in Table 1.

Table 1
PIII-treatment parameters

| Sample | Voltage (kV) | Pulse duration (μs) | Pulse frequency (Hz) | Treatment time (*h*) |
|---|---|---|---|---|
| 1 | 2.0 | 20 | 8000 | 2.5 |
| 2 | 2.0 | 20 | 8000 | 5 |
| 3 | 15 | 30 | 350–400 | 2.5 |

## 3. Results and discussion

The Auger nitrogen-depth profiles for a high voltage (HV) sample and a 2.5-h low voltage (LV) sample are shown in Fig. 2. The sputtering rate was 30 nm/min. For the LV sample, the nitrogen profile reaches a plateau region, with a concentration of about 20% at a depth of 0.2 μm, followed by a diffusion tail. The phenomenon is similar to that observed in elevated-temperature PIII experiments or high-current density-ion implantation [17–21]. In contrast, the nitrogen concentration in the HV sample is lower, and the thickness of the nitrided zone is also much smaller. We speculate that it may be caused by nitrogen out-diffusion or sputtering, in spite of a lower total-incident ion dose compared to the LV sample, and more work must be done to identify the mechanism.

The X-ray diffraction (XRD) spectra (Cu $K_\alpha$) at an incident angle of 5° are displayed in Fig. 3. The diffraction spectra acquired from the samples treated at LV reveal the formation of new phases. The broad peak near 41° is thought to be the diffraction pattern of a mixture of the expanded austenite $\gamma_N$ and $\gamma'$-$(Fe,Cr,Ni)_2N$ [11]. However, the $\gamma_N$ peak has a low intensity compared to the austenite peak. This indicates that the $\gamma_N$ phase is relatively sparse, or forms at a shallow depth. In comparison, for the 450°C sample, the primary austenite phase-diffraction pattern has almost disappeared, and only the signal corresponding to the expanded $\gamma_N$ phase exists. Thus, our data show that the formation of the $\gamma_N$ phase is more dependent on the implantation temperature. For the sample treated at HV, no new

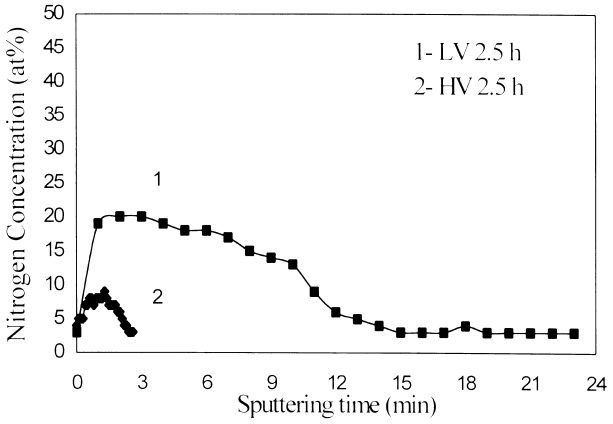


Fig. 2. Auger depth profiles of the LV and HV 2.5-h samples.

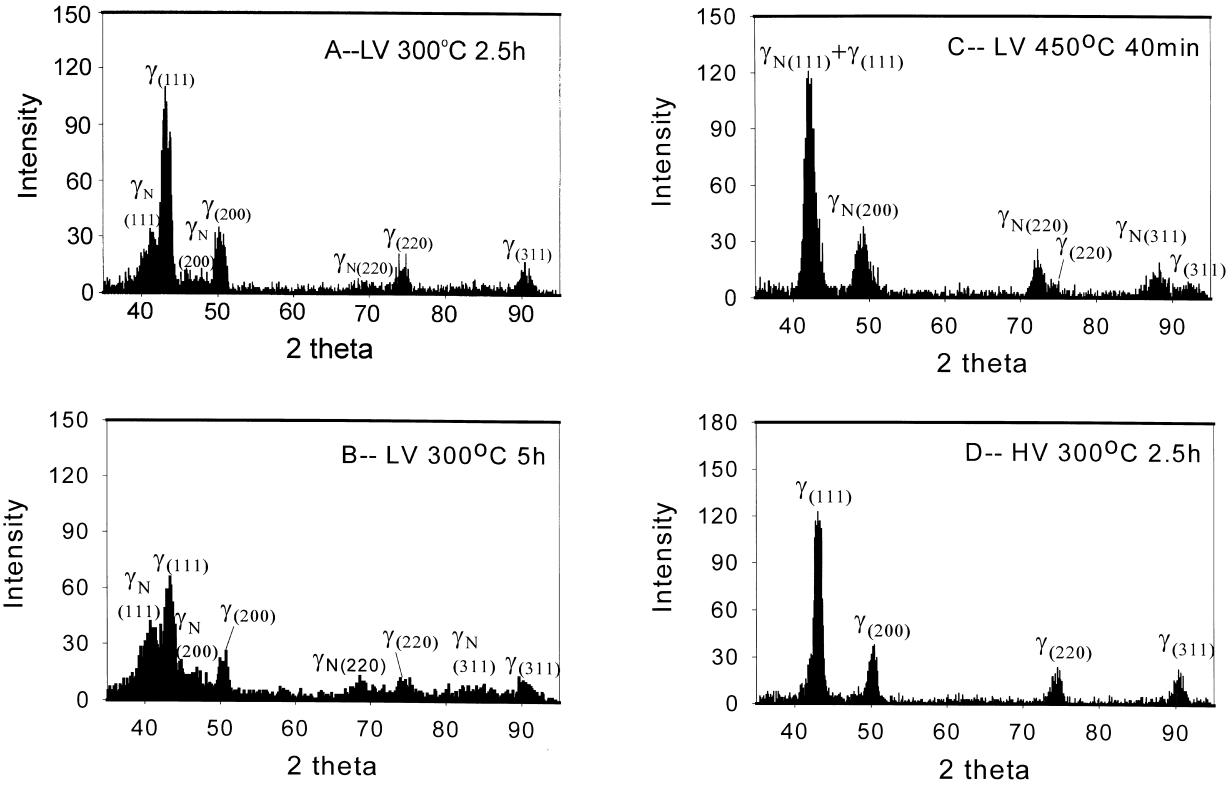


Fig. 3. Glancing XRD patterns acquired from the four samples: (A), LV, 300°C, 2.5 h; (B), LV, 300°C, 5 h; (C), LV, 450°C, 40 min; (D), HV, 300°C, 2.5 h.

phase can be detected because of the thinner modified layer and lower implant dose, as shown in Fig. 2. For the LV, 5-h sample, the $\gamma_{N(220)}$ (the peak near 70°) appears in the XRD pattern, besides the $\gamma_{N(111)}$ peak. Hence, our X-ray data illustrate that for our experimental conditions, the sample temperature is the primary factor influencing the formation of the new phase, including $\gamma_N$, followed by the implanted dose. It is mainly due to the higher incident ion-flux, facilitating rapid nitrogen diffusion to form in a thicker modified layer.

Microhardness measurements were conducted on a HX-1000 microhardness instrument, and the relationship with the applied load is demonstrated in Fig. 4. It was found that the surface microhardness of all the treated samples was enhanced significantly, especially for the LV samples. The implanted dose and diffusion time evidently influence the hardening effects. For the HV sample, the microhardness decreased quite quickly with increased applied load, and reached the same value as the untreated sample at a lower applied load, compared to the LV samples. On the other hand, the LV samples demonstrated a higher surface hardness up to a load of 500 g, indicating the formation of a thicker modified layer.

The friction and wear behavior of all the treated samples based on pin-on-disk tests were also improved as illustrated in Figs. 5 and 6. The applied load was 100 g, using a 3-mm radius silicon nitride ball. All the friction coefficient curves show a monotonic tendency, indicating a smooth modified layer produced at an elevated temperature. This is unlike the results obtained under low-temperature PIII, when a sudden 'breakthrough' was observed in the pin-on-disk test [22]. Comparing the two LV samples, the longer treatment time gave rise to a better friction behavior. The friction property of the HV sample is more superior. This can perhaps be attributed to nitrogen solution-strengthening and a greater compressive stress induced by the higher bombardment energy. Similar to the friction characteristics, the wear resistance of all the treated samples was also substantially improved, as shown in Fig. 6. However, in contrast with

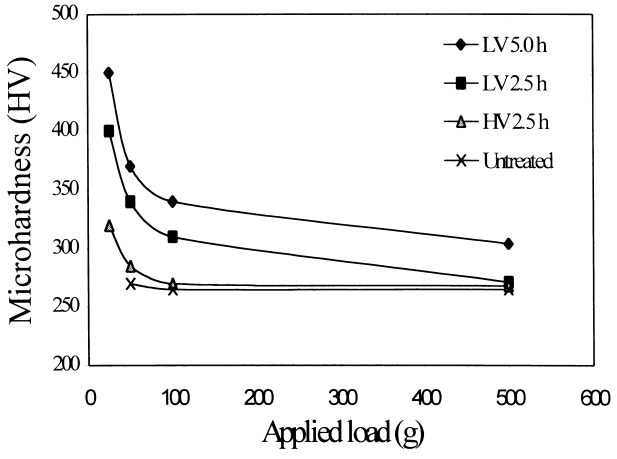


Fig. 4. Microhardness versus applied load for the four samples.

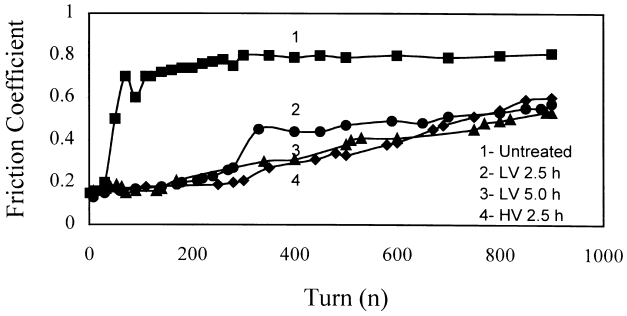


Fig. 5. Coefficients of friction versus turns in pin-on-disk tests for the four samples.

the friction results, the HV sample demonstrated a higher wear-rate than the LV samples. Among the two LV samples, a longer treatment time led to better wear resistance. In fact, the wear track-size of the 5-h sample is hardly visible and on the order of the surface roughness. Comparison of the cross-sectional area of the wear tracks shows that medium-temperature PIII gives rise to a wear-resistance enhancement of a maximum of 11.25 times in our experiments.

The potentiodynamical polarization test was performed using the Model 342 softcorrv™ corrosion-measurement system. The 2% NaCl solution was made from analytical-grade reagent and distilled water. The scanning rate was 0.5 mV/s. The measured results for the untreated, as well as treated samples, are shown in Fig. 7. After plasma treatment, the corrosion potential was unequivocally increased, and the polarization curves shifted to the left compared to that of the untreated sample, implying an improvement in the corrosion resistance. The corrosion potential of the untreated sample was about −400 mV, whereas that of all the treated samples was higher at −200 mV. This can be explained by the formation of the $\gamma_N$-phase in the LV samples, and the HV treatment helps to stabilize the protective oxide layer on the surface [23]. The polarization curves show that a LV process yields better corrosion resistance.

Our data unequivocally demonstrate that medium-

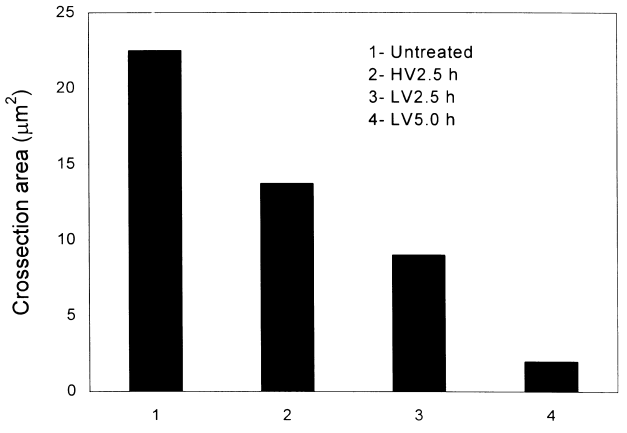


Fig. 6. Wear track cross-sectional areas obtained after 900 turns at a loading of 100 g.

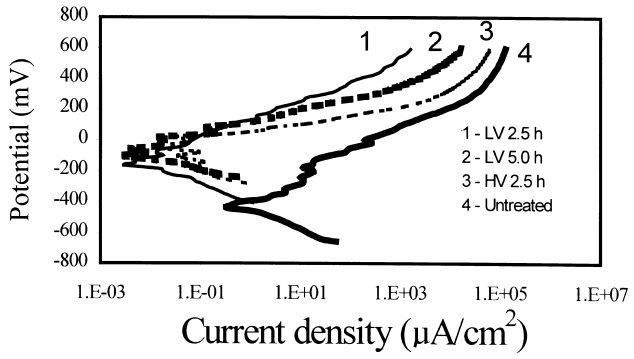


Fig. 7. Potentiodynamic polarization curves obtained in a solution of 2 wt.% NaCl.

temperature PIII leads to a considerable improvement in both the wear and corrosion resistance of SS304 stainless steels. New phases, consisting of a mixture of expanded austenite and $\gamma'$-$(Fe,Cr,Ni)_2N$, were formed in the modified layer of the LV samples. This structure is quite different from that obtained using low-pressure ion nitriding [24]. In previously reported results, the main components of the nitrided layer were $\varepsilon$-$Fe_3N$ and $(Fe,Cr)_2N$, and the primary austenite peak was absent. We suspect that it was due to hydrogen as a carrier gas and the higher working pressure of 10–15 mTorr. In our experiments, no new phase was observed in the HV sample. Nonetheless, regardless of the operating mode, the corrosion resistance of all of the treated samples was improved, as demonstrated in Fig. 7.

The LV sample with a longer implantation time has the best wear-resistance property, which can be ascribed to deeper diffusion of implanted nitrogen. Our AES data show that the retained dose of the LV sample is considerably more than that of the HV sample. In situations when no external heating is supplied and the sample is only heated by the incident ion-flux, the LV mode is better due to its higher incident flux. In contrast, in the HV process, the implantation rate must be reduced to maintain the pre-determined treatment temperature [25,26], thereby leading to thinner layers, and hence, lower microhardness and higher wear-rate.

## 4. Conclusion

PIII of SS304 austenitic stainless steel was conducted at a medium temperature of 300°C, using both high and LV modes. Our data show that medium-temperature PIII treatment results in an improvement in both the wear and corrosion resistance, and the LV process yields more superior tribological and corrosion-resistance properties. The difference between the two modes may be due to the ion-flux and the retained dose. Thus, our data show that a higher implantation flux (that is, a higher implanted dose for the same treatment time) is more crucial than a high implantation voltage.

## Acknowledgements

The work was supported by the Hong Kong Research Grants Council Earmarked Grants 9040332, 9040344 and 9040412, City University of Hong Kong Strategic Research Grant 7000964, and RGC/Germany Joint Scheme 9050084.

## References

[1] J.R. Conrad, J.I. Radtke, R.A. Dodd, F.J. Worzala, N.C. Tran, J. Appl. Phys. 62 (1987) 4591.
[2] P.K. Chu, S. Qin, C. Chan, N.W. Cheung, L.A. Larson, Mater. Sci. Eng. Rep. R17 (1996) 207.
[3] B.Y. Tang, P.K. Chu, S.Y. Wang, K.W. Chow, X.F. Wang, Surf. Coat. Technol. 103–104 (1998) 248.
[4] S.Y. Wang, P.K. Chu, B.Y. Tang, X.B. Tian, X.F. Wang, Q.Z. Lin, Thin Solid Films 311 (1997) 190.
[5] S.Y. Wang, P.K. Chu, B.Y. Tang, J.C. Yan, X.C. Zeng, Surf. Coat. Technol. 98 (1998) 897.
[6] M. Samandi, B.A. Shedden, T. Bell, G.A. Collins, R. Hutchings, J. Tendys, J. Vac. Sci. Technol. B 12 (1994) 935.
[7] G.A. Collins, R. Hutchings, K.T. Short, J. Tendys, X. Li, M. Samandi, Surf. Coat. Technol. 74/75 (1995) 417.
[8] C.B. Franklynand, G. Nothnagel, J. Vac. Sci. Technol. B 12 (1994) 923.
[9] C. Blawert, B.L. Mordike, G.A. Collins, K.T. Short, J. Tendys, Surf. Coat. Technol. 103/104 (1998) 240.
[10] S. Mandl, R. Gunzel, E. Richter, W. Moller, Surf. Coat. Technol. 100/101 (1998) 372.
[11] M.K. Lei, Z.L. Zhang, J. Vac. Sci. Technol. A 15 (1997) 421.
[12] P.J. Wilbur, B.W. Buchholtz, Surf. Coat. Technol. 79 (1996) 1.
[13] P.K. Chu, B.Y. Tang, Y.C. Cheng, P.K. Ko, Rev. Sci. Instrum. 68 (1997) 1866.
[14] X.B. Tian, Z.N. Fan, X.C. Zeng, Z.M. Zeng, B.Y. Tang, P.K. Chu, Rev. Sci. Instrum. 70 (1999) 2818.
[15] X.B. Tian, X.F. Wang, B.Y. Tang, P.K. Chu, P.K. Ko, Y.C. Cheng, Rev. Sci. Instrum. 70 (1999) 1824.
[16] X.B. Tian, X.F. Wang, S.Y. Wang, B.Y. Tang, P.K. Chu, in: A. Kumar, Y.W. Chung, J.J. Moore, J.E. Smugeresky (Eds.), Surface Science and Technology I Proceedings, 1999 TMS Annual Meeting, 1999, p. 177.
[17] R. Wei, B. Shogrin, P.J. Wilbur, O. Ozturk, D.L. Williamson, I. Ivanov, E. Metin, J. Tribol. 116 (1994) 870.
[18] D.L. Williamson, J.A. Davis, P.J. Wilbur, J.J. Vajo, R. Wei, J.N. Matossian, Nucl. Instrum. Methods B 127/128 (1997) 930.
[19] R. Wei, Surf. Coat. Technol. 83 (1996) 218.
[20] C. Blawert, A. Weisheut, B.L. Mordike, F.M. Knnop, Surf. Coat. Technol. 85 (1996) 15.
[21] M. Samandi, B.A. Shedden, D.I. Smith, G.A. Collins, R. Hutchings, J. Tendys, Surf. Coat. Technol. 59 (1993) 261.
[22] A. Chen, J. Blanchard, J.R. Conrad, P. Fetherston, X. Qiu, Wear 169 (1993) 97.
[23] R. Hutchings, W.C. Oliver, Wear 92 (1983) 143.
[24] E.I. Meletis, S. Yan, J. Vac. Sci. Technol. A 11 (1993) 25.
[25] S. Leigh, M. Samandi, G.A. Collins, K.T. Short, P. Martin, L. Wielunski, Surf. Coat. Technol. 85 (1996) 37.
[26] G.A. Collins, R. Hutchings, K.T. Short, J. Tendys, Surf. Coat. Technol. 103/104 (1998) 212.